Robust Tracking and Control Strategies for Automatic Landing Systems

MICHAEL J. ROEMER

An automatic landing system (ALS) for aircraft is discussed and analyzed to emphasize possible procedures for enhancing the performance of aircraft tracking and control strategies. Techniques such as control/filter variable optimization and noise filtering are introduced as incentives for the development of an ALS for commercial aircraft. The robust nature (less sensitive to noise and disturbance) of the tracking and control algorithms is advantageous for adverse weather conditions and noise-corrupted radar measurements. Improvements attributed to these tracking and control concepts are demonstrated on a closed-loop computer simulation of an aircraft under automatic control. Robust automatic landing systems utilizing these strategies will prove to be essential in the design of aircraft control systems proposed for accurate terminal-area automatic landings.

Consider an automatic landing system (ALS) for commercial aircraft that would allow for safer and more efficient airspace management or an advanced guidance and control scheme for military combat aircraft that would permit leaving the pilot home under extremely hazardous situations. Are these aviation goals for automatic control possible? Definitely, considering the projected advances in computer technologies that will shape the automated control industry of the future. Full integration of the many aspects of aircraft control, in particular those associated with robust (less sensitive to noise and disturbance) tracking and control methodologies, is a first step to reaching these goals.

The Microwave Landing System (MLS) is the new international standard landing aid planned to replace the current Instrument Landing System (ILS) as early as 1995. The MLS will be capable of determining the position of an aircraft in three-dimensional space over a large coverage area, and it is less sensitive to surrounding interference than the ILS. Some of the operational benefits of the MLS include (a) use of curve/segmented approaches, (b) use of back azimuth guidance, (c) use of higher glide slopes/reduced siting problems, (d) relief of frequency congestion, and (e) increased reliability and maintainability (*1,2*). The MLS, however, is an advanced guidance system in which no direct, automatic control of the aircraft is performed. The focus of this paper is the development and simulation of some robust features associated with ALSs that could contribute to the evolution of a future ALS for commercial aircraft.

There are many unanswered questions about the technical feasibility of an ALS for civilian aircraft. The current ALSs used by naval aircraft carriers utilize ground-based, lock-on-type radar, whereas current civilian technology includes MLS and satellite procedures. The main difference is that MLS and satellite technologies are not fast enough for the required frequency of position updates needed for automatic control in the current system. The author does not propose to overcome the inertia of the current civilian technology. However, possible alternatives include (a) developing a separate, ground-based ALS to supplement MLS technologies, (b) using accurate estimation techniques that predict aircraft position between radar measurements, and (c) waiting for the advances in computer technologies so that the required position updates can be obtained. Regardless of the alternative, the future development of an ALS for commercial aircraft must remain an option for aviation policy makers.

Assuming that the option for civilian ALSs is feasible, the performance of the tracking and control strategies of a ground-based ALS are investigated. A computer simulation that accurately represents an operating ALS is necessary for testing possible improvement techniques. The essential computer simulation blocks contained in an ALS are the tracking filter, the controller, and the aircraft model. These simulation blocks are introduced, analyzed, and then combined in a closed-loop simulation to model an aircraft under a particular ALS control. This closed-loop performance is carefully analyzed in the frequency and time domains and compared with actual measurements taken during a test flight to ensure compatibility. Once the basic ALS background is established, some possible areas of improvement are examined. An area of particular interest, highlighted in a later section, is the ALS's noise rejection capabilities.

To decrease the noise sensitivity of a generalized ALS, a filtering technique utilizing both measurement data and modeled aircraft dynamics is introduced. The proposed filter blends information obtained by radar measurements with aircraft model estimates to produce a less noise-sensitive pitch command, which in turn is sent to the aircraft to control it. The proposed noise rejection filter equations are explained in detail later. After the filter is included in the computer simulation, a complete frequency and time domain analysis is performed and compared with the simulation without the filter. The filter produces the desired reduction in noise sensitivity. However, this desirable reduction is obtained at the cost of an undesirable increase of the turbulence response of the aircraft.

To address the concern of an increased turbulence response, the author approached the problem using optimization techniques. The optimization problem consists of the minimization of a cost function related to (a) the turbulence response of an aircraft and (b) the unit step response of the aircraft. The optimization of the cost function is with respect to the control gains as well as the tracking filter gains. After cal-

Department of Mechanical and Aerospace Engineering, State University of New York at Buffalo, Buffalo, N.Y. 14260.

culation of the optimal control and filter gains for a particular weighting, the complete ALS simulation is tested to ensure an improved solution.

GENERALIZED ALS

First, the procedures and equations necessary for the construction of an ALS computer simulation are discussed. For the purpose of organization, the simulation can be classified into three parts: aircraft model, tracking filter, and controller.

Aircraft Model

Creating a concise mathematical model of the dynamics of an aircraft for computer simulation is not a trivial procedure. The sophistication levels can range from a coupled 12th-order state-space representation of the familiar equations of motion to a simple transfer function model utilizing an integration procedure. For the purposes of evaluating tracking filter performance and control schemes in a closed-loop ALS simulation, a relatively small-order model is sufficient. The underlying procedure used in the construction of the aircraft model is to match the dynamic response characteristics of actual aircraft data measured through flight testing (*3*). The measurements come from an F-4 fighter plane and consist of frequency domain data for a transfer function relating altitude to pitch command. For a commercial aircraft, the mathematically modeled differences would consist of slower time constants (denominator) and a larger overall gain (numerator). The F-4 was used in the modeling process because of the availability of the data for comparison purposes. For simplification reasons, the aircraft model transfer function used in the generalized ALS computer simulation is as follows:

$$\frac{Z(s)}{\Theta_c(s)} = \frac{G}{s(1 + t_1 s)(1 + t_2 s)} \tag{1}$$

where

$Z(s)$ = aircraft altitude,
$\Theta_c(s)$ = pitch command signal,
G = constant gain, and
t_1, t_2 = time constants.

This simplified aircraft transfer function is a single-input, single-output (SISO) relationship. The input signal is the pitch command calculated by the controller, and the output signal is the aircraft altitude. The obvious question that arises is, what happens to the other aircraft states that are in theory coupled with the pitch command signal to control the aircraft? The answer is found by decoupling the equations of motion. Decoupling the states associated with the control of aircraft is a common practice often performed in industry to simplify the design criteria and retain robust stability. In this case, the aircraft model only gives information about the aircraft altitude. However, if information about the lateral position of the aircraft is desired, a more advanced transfer function matrix could be substituted. This was not considered here because a simplified aircraft model was desired.

The aircraft model's transfer function consists of a second-order pole with time constans of $t_1 = 1.0$ and $t_2 = 1.4$ sec multiplied by an integrator with constant gain of $G = 5.0$. However, to more practically represent the motions of an aircraft, turbulence must be added to the transfer function. The block diagram of the transfer function with this addition is shown in Figure 1.

The integrator acts to produce the elevation changes in the aircraft, whereas the two poles approximate the cut-off frequencies associated with elementary aircraft motions. The aircraft transfer function was digitally simulated using a fourth-order Runge-Kutta numerical integration technique. The output states represent close approximations of the aircraft altitude and its first and second derivatives. This transfer function is a good imitation to measured data obtained during an aircraft test flight (*3*).

Tracking Filter

A state estimation filter that aids in aircraft tracking is examined in this section. Assuming that the aircraft's position is the only radar measurement currently available, aircraft tracking would be performed by processing noisy position measurements only. A great deal of effort has been concentrated on producing suboptimal filters with reduced computational requirements (*4–9*). This type of filter is used for examining the noise sensitivity of the generalized ALS discussed in this paper. With this in mind, a basic α-β-γ filter is designed as part of the ALS computer simulation to assist in estimating the prominent states of the aircraft.

Similar to most digital filters, the output of the α-β-γ filter is based on a weighted average between a current measurement and an estimated prediction. The estimated prediction is calculated using previous output measurements. For the ALS under investigation, the digital filter precedes the standard control algorithms. Derivative (D) and double derivative (DD) control is necessary to obtain useful velocity and accel-

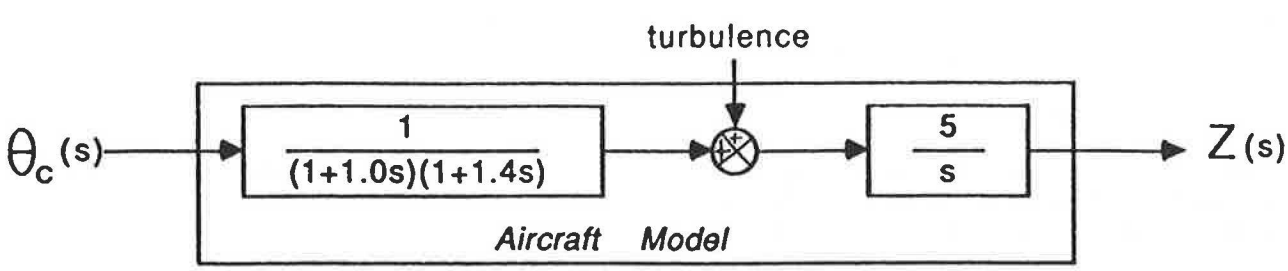

FIGURE 1 Aircraft transfer function block diagram.

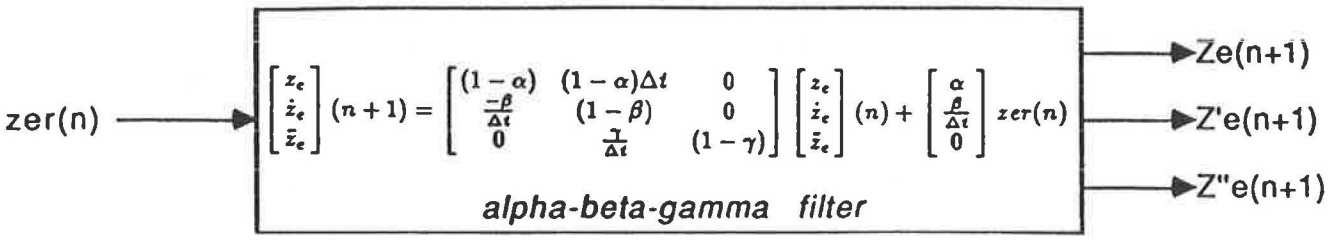

FIGURE 2 Tracking filter block diagram.

eration error estimates. This technique of filtering the error signal of the position measurement is illustrated in Figure 2. The position error signal is the difference between the command trajectory and the actual aircraft position obtained by radar.

The α-β-γ filter equations are derived in the following manner. First, a predicted error signal $z_e^p(n)$ is derived using a discrete time, truncated Taylor series:

$$z_e^p(n) = z_e(n-1) + \Delta t \dot{z}_e(n-1) \tag{2}$$

where n and $n-1$ are the current and previous discrete times.

Utilizing the filtering idea of a weighted average, the predicted error signal $z_e^p(n)$ and the current position error measurement signal $zer(n)$ are combined in the following manner to produce the output signal $z_e(n)$.

$$z_e(n) = (1-\alpha)z_e^p(n) + \alpha zer(n) \tag{3}$$

where α is the weighting gain for position error measurement.

In similar fashion, the first derivative of the filtered error signal is calculated by combining the previous velocity estimate with a numerical estimate of the derivative. The equation used in its calculation is the following:

$$\dot{z}_e(n) = (1-\beta)\dot{z}_e(n-1) + \beta\left[\frac{zer(n) - z_e(n-1)}{\Delta t}\right] \tag{4}$$

where β is the weighting gain for the velocity error estimate.

The acceleration section of the α-β-γ filter is separated into two equations. The first equation serves as an intermediate step to the calculation of the second derivative of the filtered error signal. This equation is written as follows:

$$\ddot{z}_e'(n) = (1-\gamma)\ddot{z}_e(n-1) + \frac{\gamma}{\Delta t}\left[\dot{z}_e(n) - \dot{z}_e(n-1)\right] \tag{5}$$

where γ is the weighting gain for the acceleration error estimate.

The second derivative of the filtered error signal is then calculated using the previous equation, and is shown below:

$$\ddot{z}_e(n) = \ddot{z}_e(n-1) + \gamma[\ddot{z}_e'(n) - \ddot{z}_e'(n-1)] \tag{6}$$

A performance evaluation of the α-β-γ filter equations was conducted. The analysis can be broken down into two sections. First, a gaussian distributed random signal with mean ($\mu \approx 0.0$) and variance ($\sigma^2 \approx 1.0$) was used to test the transient and steady-state responses of the filter. The values of μ and σ were chosen to represent a possible error signal between the desired and actual aircraft measurements. Next, two sine waves with frequencies of 4.0 and 0.8 rad/sec were used as inputs to check the phase lag in the filter. It was concluded that if there was a significant transient input to the filter, the filter would adjust to it within 1 sec (*3*).

Controller

A commonly implemented control strategy often utilizes proportional (P), integral (I), derivative (D), and second derivative (DD) control methodologies. This type of controller was chosen so that the best possible combination of classical control techniques could be implemented. Also, additional filtering is often desirable at the output of such conventional control algorithms. For instance, a simple first-order low-pass filter could be used to protect against severely changing control signals. This robust filter-controller algorithm is designed to withstand the most intense turbulence and to eliminate the possibility that the controller might produce a control signal that forces the plane to become unstable.

The PIDDD controller equations implemented in the general ALS computer simulation are formulated in the following manner. First, the equations are illustrated in block diagram form (Figure 3) and then written in a discrete time format.

The discrete time integral action is derived by summing a weighted average of the previous integral signal with a numerical integration approximation. This equivalence is shown below:

$$\Theta_{INT}(n) = \Theta_{INT}(n-1) + \frac{K_0}{K_I}\left[\frac{z_e(n) + z_e(n-1)}{2}\right]\Delta t \tag{7}$$

where $\Theta_{INT}(n)$ is the integral control action.

This result is then used along with the filtered error signal and its derivatives to produce the following control signal:

$$\begin{aligned}\Theta'_c(n) = {} & K_0[K_P z_e(n) + K_D \dot{z}_e(n) \\ & + K_{DD}\ddot{z}_e(n)] + \Theta_{INT}(n)\end{aligned} \tag{8}$$

where

K_0 = encompassing gain constant,
K_P = proportional control gain,
K_I = integral control gain,
K_D = derivative control gain, and
K_{DD} = double derivative control gain.

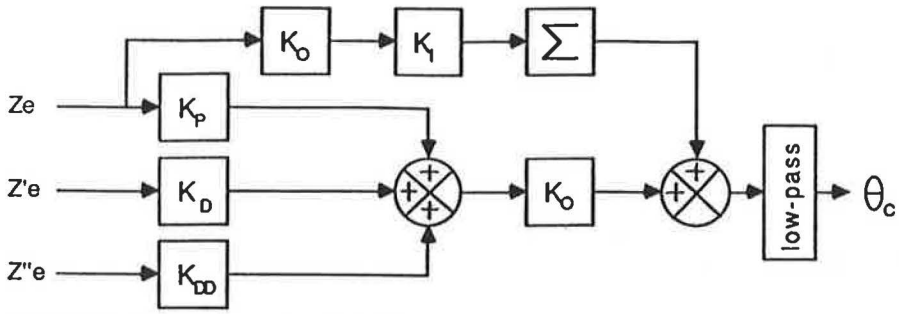

FIGURE 3 PIDDD controller block diagram.

The calculated $\Theta'_c(n)$ control signal is then used as an input to the low-pass filter to produce the actual control signal $\Theta_c(n)$,

$$\Theta_c(n) = \Theta_c(n-1) + \alpha_p[\Theta'_c(n) - \Theta_c(n-1)] \tag{9}$$

where α_p is the $(\Delta t)\omega_c$, and ω_c is the break point frequency.

CLOSED-LOOP COMPUTER SIMULATION

Attention is now focused on the closed-loop integration of the simulation blocks discussed in the previous section. The blocks of a general ALS model are arranged into the closed-loop configuration shown in Figure 4.

This closed-loop ALS is designed to control the vertical position of an approaching aircraft until it lands safely. The position error signal characterized by the aircraft's vertical position is the input to the filter. The output contains estimates of the aircraft's altitude error and its first and second derivatives. The output error estimates of the α-β-γ filter are used as inputs to a PIDDD controller scheme. The controller is responsible for producing an unpolished pitch command signal that, in refined form, will be communicated to the aircraft to produce a desired vertical position. Finally, the current position of the aircraft is tracked by the radar system and fed back to the ALS to begin the cyclic process again. This closed-loop signal processing continues until the aircraft has landed.

Frequency and time domain analysis was employed to fully investigate the compatibility of the general ALS's computer simulation with practical operating conditions. First, a frequency domain approach is used to compare the resulting computer simulation with actual test flight data, followed by an examination of the time domain step response to ensure proper closed-loop behavior. Then, simulated noise and turbulence are added to the simulation to examine noise sensitivity and turbulence response.

Frequency Domain Characteristics

An excellent means of confirming whether the closed-loop simulation is operating properly is to compare it with some actual test flight measurments. Through the use of a Nichol's chart, an available set of open-loop frequency test flight data is transformed into a closed-loop Bode plot. Next, the closed-loop simulation is subjected to sinusoids of several different frequencies in order to construct the computer-simulated Bode plot. The results of the simulated frequency domain analysis are plotted together with the test flight data to ensure compatibility. These plots appear in Figures 5 and 6.

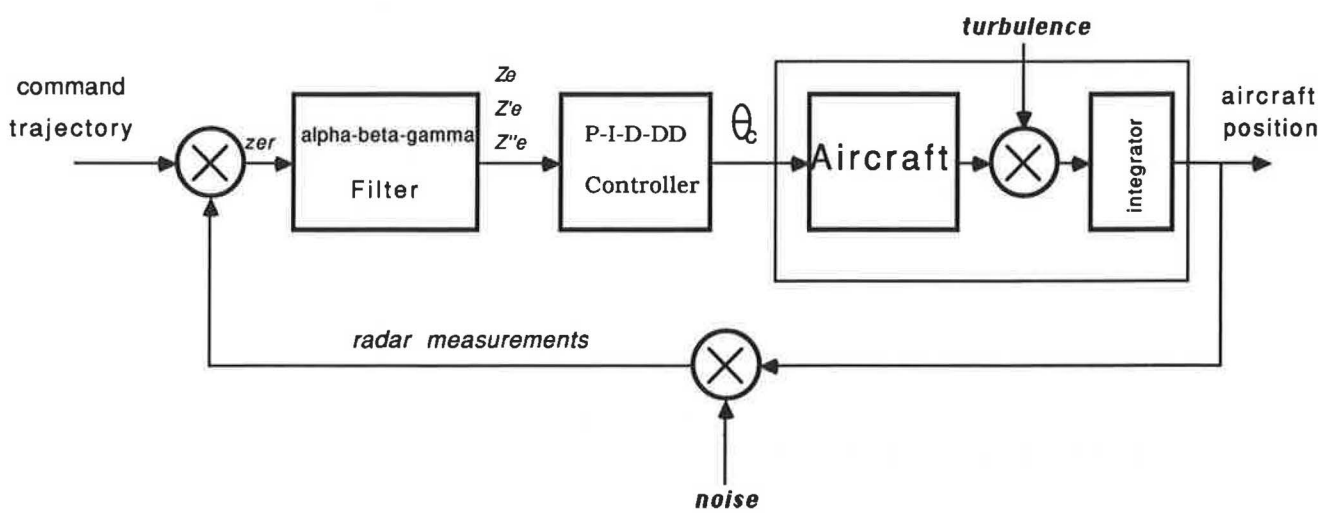

FIGURE 4 Automatic landing system block diagram.

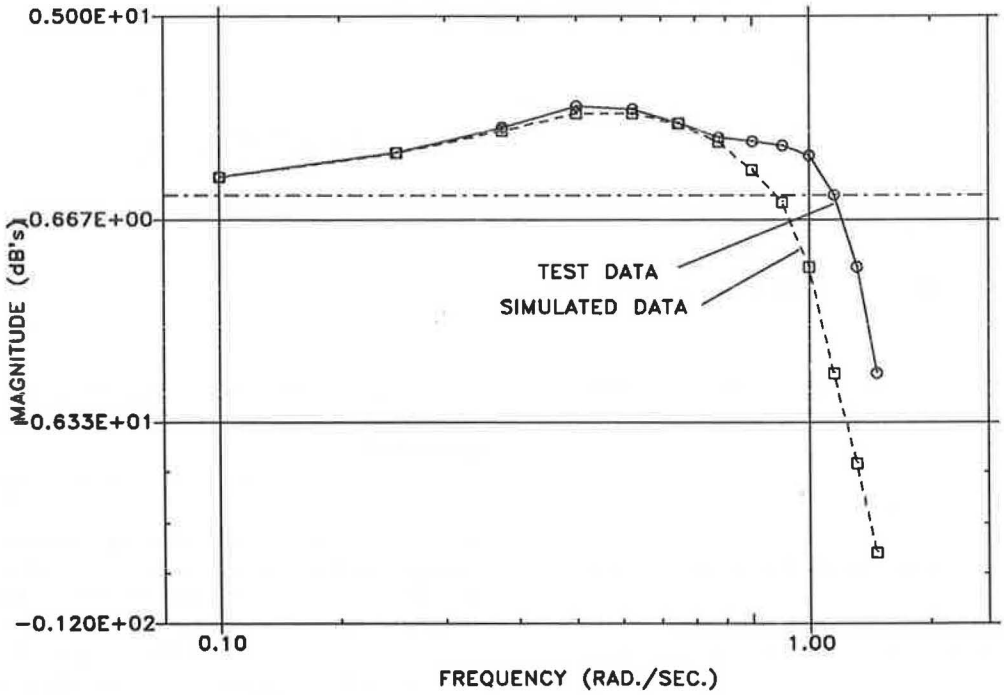

FIGURE 5 Magnitude Bode plot comparison.

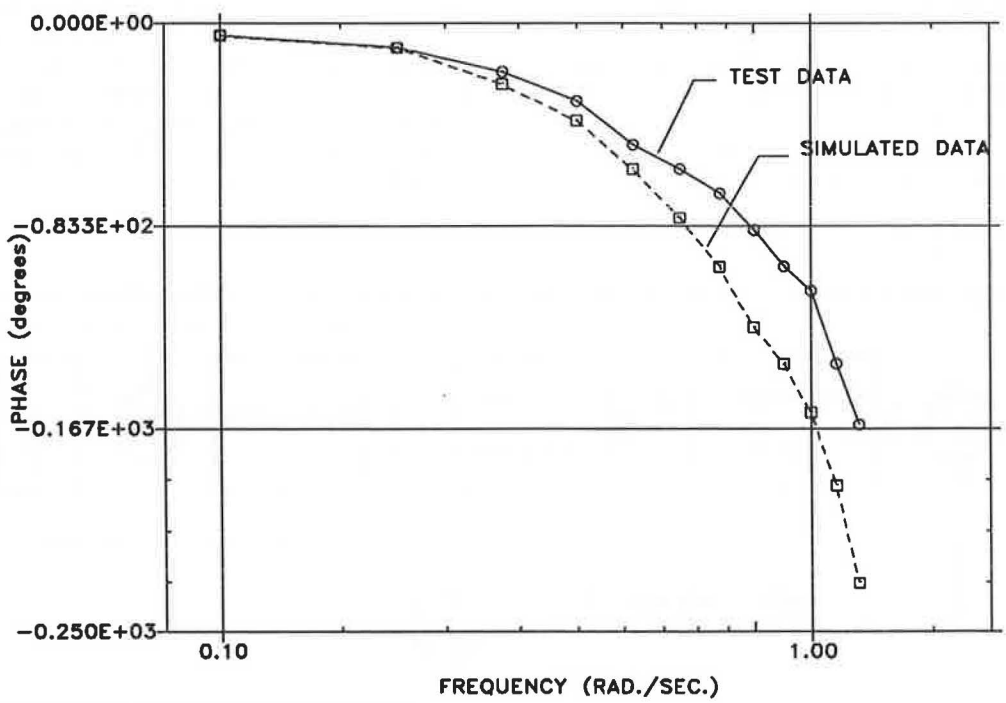

FIGURE 6 Phase Bode plot comparison.

Time Domain Considerations

Time domain analysis, in particular the step and turbulence responses, is a widely used graphic tool for designing various types of aircraft controllers. Design characteristics associated with the step response, such as rise time, overshoot, and settling time, are often considered the most significant results when the performance of a control system is rated. Moreover, obtaining a minimal turbulence response with respect to a given trajectory is often desirable when the turbulence response of an aircraft is examined. Examining the step response of the ALS simulation reveals an overshoot of 5.0 percent, a rise time of 5 sec, and a settling time (± 5 percent of steady-state value) of 20 sec. This step response incorporates a fine balance between the integral and derivative control gains that controllers of all robust landing systems must acquire. The gains must be structured enough to keep an airplane from suffering rapidly changing motions and flexible enough to allow for a quick response time.

To better represent the practical operation of the ALS, simulated radar noise and turbulence are introduced into the closed-loop simulation. As shown in Figure 4, the turbulence is added directly to the aircraft transfer function, whereas the noise is added to the position measurements of the aircraft. Turbulence is normally a result of air temperature instabilities and adverse weather conditions. Noise can include such complex ingredients as electromagnetic interference (EMI) from the radar system or any combination of measurement uncertainties. Therefore, the ability of a landing system to maintain tight control in the presence of noise and turbulence is of primary importance.

Althogh exact models predicting the nature and magnitude of the noise and turbulence present in the ALS are not obtainable, experimentally tested approximations used by the U.S. Navy are employed. First, an approximation of the noise that corrupts the position measurements of the radar tracking device is discussed. Normally, the most troublesome noise a landing system encounters is that in which the frequency content of the noise is located in the system's normal operating frequency bandwidth. Therefore, simply using a sine wave with a frequency near that of the system's operating frequency is assumed to be sufficient. The simulated ALS's frequency bandwidth ranges from approximately 0.1 rad/sec to 5 rad/sec. Next, a digital representation of turbulence is approximated by low-pass filtering a gaussian distributed random signal with zero mean. For this approximation, a commonly used cut-off frequency for the filter is 0.30 rad/sec. This is consistent with actual aircraft data (*3*).

The turbulence response of an aircraft can be defined as the relative position of the aircraft when the command (reference) signal is zero and only outside disturbances (noise and turbulence) affect the system. The generalized ALS, without noise rejection capabilities, has the turbulence response and corresponding error signal shown in Figure 7. Examining the turbulence response reveals that the error signal (which is directly related to the control signal) contains a high degree of noise. Therefore, the problem with the ALS is its inability to reduce the amount of noise present in the error (or control) signal while preserving the closed-loop response of the aircraft. Next, a method is presented for improving the noise rejection capabilities of the ALS.

CLOSED-LOOP SIMULATION WITH NOISE REJECTION FILTER

This section is concerned with the design of a noise rejection filter and its resulting effects on the closed-loop response of

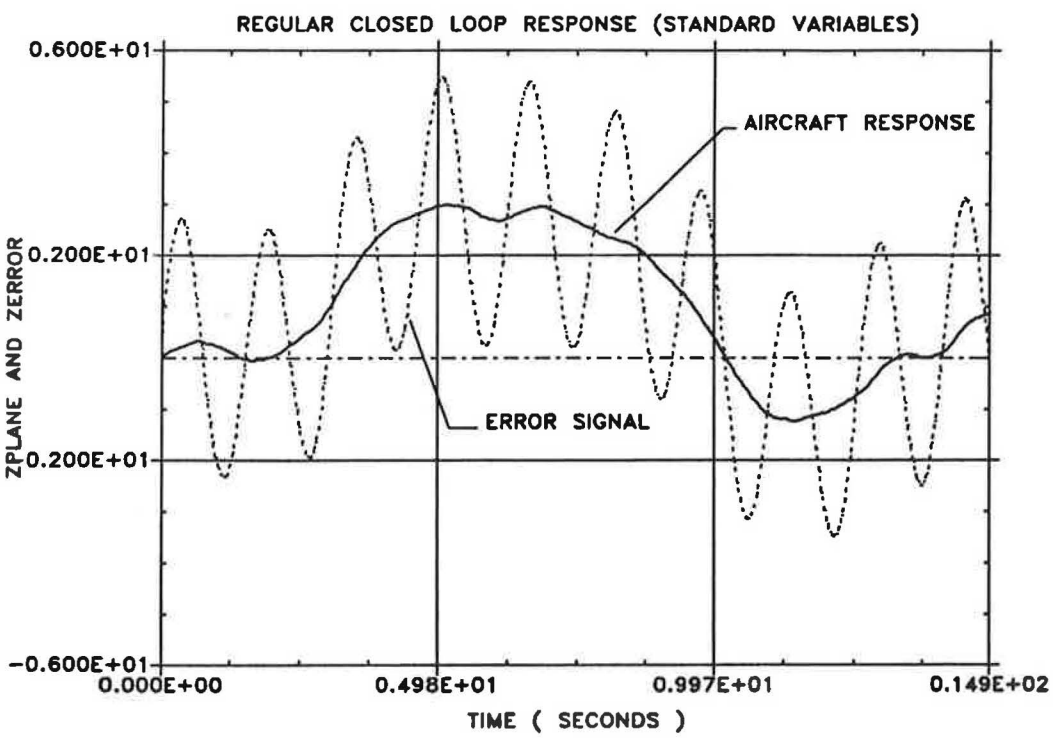

FIGURE 7 Turbulence response of ALS closed-loop simulation.

the ALS. First, a derivation of the theory involved in the development of the filter is examined. Next, frequency and time domain analysis of the total closed-loop response is used to investigate the critical characteristics of the landing system (with and without the noise rejection filter). Finally, some conclusions are drawn from the effects of the noise rejection filter on the ALS.

Noise Rejection Filter

The primary incentive for developing a noise rejection filter as part of the ALS is to reduce the amount of noise present in the control signal sent to the aircraft. This success will "smooth the bumps" in the control signal, and therefore produce more stable motions for the aircraft's response. Ideally, the effects of all radar noise should be minimized and the motion caused by turbulence should continue to be limited (preservation of the turbulence response).

The proposed noise rejection filter blends the combination of radar positional measurements with model estimates of the aircraft's velocity and acceleration to produce an error signal that is less sensitive to radar noise. The aircraft model estimates are produced from the numerical integration of the model previously developed. A transfer function representation of the proposed noise rejection filter is given as

$$Y(s) = \frac{X(s)}{s^2 + 2\zeta\omega s + \omega^2} + \frac{\Phi\hat{\dot{x}} + \Psi\hat{\ddot{x}}}{s^2 + 2\zeta\omega s + \omega^2} \tag{10}$$

where

$Y(s)$ = filter output,
$X(s)$ = measured position data,
$\hat{\dot{x}}$ = velocity estimate from aircraft model,
$\hat{\ddot{x}}$ = acceleration estimate from aircraft model, and
$\Phi, \Psi, \zeta, \omega$ = variable gains of the filter.

The corresponding time domain equivalent, which is the basis of the discrete-time simulation, can be described by the following equation:

$$y(t) = \int_0^t \int_0^t \omega^2[x(\tau) - y(\tau)]d\tau - \int_0^t 2\zeta\omega y(\tau)d\tau + \int_0^t \int_0^t \Phi\omega^2\hat{\dot{x}}(\tau)d\tau + \int_0^t \int_0^t \Psi\omega^2\hat{\ddot{x}}(\tau)d\tau \tag{11}$$

One of the underlying themes of this filter design is to assume that the equivalences $\hat{\dot{x}} \equiv s$ and $\hat{\ddot{x}} \equiv s^2$ are approximately true. Employing these assumptions and matching the numerator with the denominator, the relationships $\Phi = 2\zeta/\omega$ and $\Psi = 1/\omega^2$ are obtained. Therefore, it can easily be verified that the magnitude response of the filter should be close to unity while a blend of aircraft dynamics and measurements is performed.

The implementation of the filter's equations can be described in the following manner. First, the control signal that is sent to the aircraft is sampled at an arbitrary rate and used as input to the aircraft model. The model will in turn produce estimates of the velocity and acceleration of the aircraft. Next, the estimates and position measurements are blended to produce an error signal that is less sensitive to noise in the measurements. Therefore, the improved error signal will create a "smoother" control signal, which will in turn yield a more stable aircraft motion. The actual position of the noise filter with respect to the regular closed-loop system is shown in the block diagram in Figure 8. Because of the position of the filter, it is commonly referred to in the control literature as a model-following filter.

The parameters Φ, Ψ, ζ, and ω of the noise filter were chosen to minimize the amount of noise present in the control signal and allow the motion of the aircraft due to turbulence to pass through. Examining the parameters, the transfer function will produce a gross effect equivalent to 1 for the magnitude response of the filter. However, simultaneously these

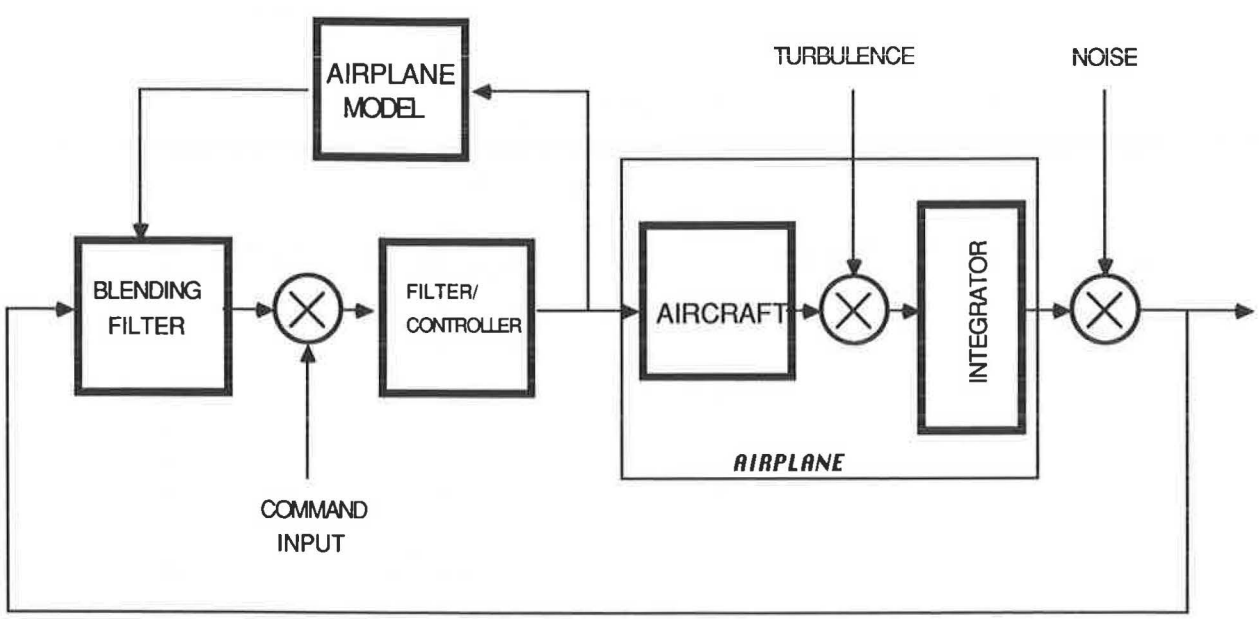

FIGURE 8 Closed-loop block diagram with noise filter.

parameters directly affect the measurement or estimate present in the blended error signal. For example, if ω equals 0.10, the modeled aircraft dynamics become the dominant factor in the blended error signal. However, for a value of ω equal to 10.0 the emphasis is placed on the position measurements.

It is equally important to choose these parameters in order to obey the classical control laws of a second-order system. For example, the denominator of the transfer function (called the characteristic equation) should produce roots (poles) that yield a proper damping ratio and natural frequency consistent with a stable system. Thus, choosing to model a system with ω equal to 1 rad/sec and a damping ratio of 0.7 produces the parameters $\Phi = 1.4$ and $\Psi = 1.0$. These are the parameters used in the simulation of the ALS.

An example of the noise rejection capabilities of the proposed filter is shown in Figures 9 and 10. First, using only noise as the input disturbance, a command signal of zero was directed to the aircraft. A plot of the input noise, control signal, and aircraft response for the case of no noise rejection filter is given in Figure 9. Under identical conditions, the simulation including the noise rejection filter was tested, and the resulting plot is given in Figure 10. The disturbance response of the aircraft utilizing this noise rejection (model-following) filter is obviously much less than that with no filter. These results illustrate the advantage for employing this filter in the basic ALS.

Filter Analysis

The generation of frequency domain Bode plots for the closed-loop system with a noise rejection filter was conducted in a manner similar to that described earlier. Sinusoids of several different frequencies with a magnitude of 1 were used as inputs to the discrete time simulation. Then the steady-state output was observed to determine the magnitude and phase changes in the signal. A summary of the closed-loop characteristics obtained from the Bode plots of both simulations is given in Table 1. It is apparent that there is a small increase in the magnitude response for the simulation with the noise filter.

To further examine the properties of this closed-loop simulation with a noise rejection filter, an investigation of the time domain characteristics is conducted. The time domain step response properties of both simulations are given in Table 2. Similar to the frequency domain results, the characteristics are almost identical except for the percentage of maximum overshoot. This supports an inclination that an increased aircraft response exists when the noise rejection filter is employed.

Judging from the relative increases in the response of the aircraft from the previous frequency and time domain analysis, one might predict that the turbulence response of the aircraft is also magnified. The turbulence response, using the identical noise and turbulence disturbance inputs, is in fact increased by almost a factor of 2. However, the great reduction of noise sensitivity in the control signal due to this filtering must not be forgotten. The graph of the turbulence response with the noise rejection filter is shown in Figure 11.

It can be deduced, by comparing Figures 7 and 11, that despite the successful reduction of the noise sensitivity of the control signal, the noise filter did not preserve the motion of the aircraft due to turbulence. Therefore, the question of how to decrease this turbulence response and simultaneously reject the noise using the proposed filter must be addressed. A simple solution to the problem might be to eliminate the use of the filter and try something different. However, because of the excellent noise rejection capabilities of the filter, an alternative solution would be more advantageous. One pos-

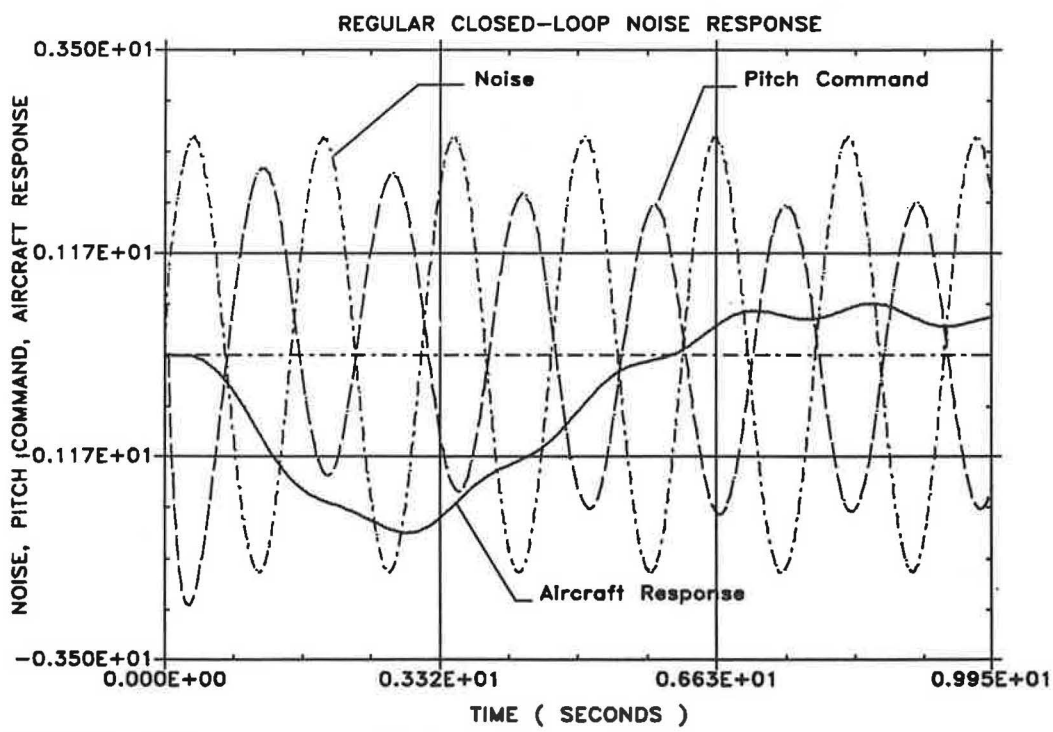

FIGURE 9 Disturbance response without noise filter.

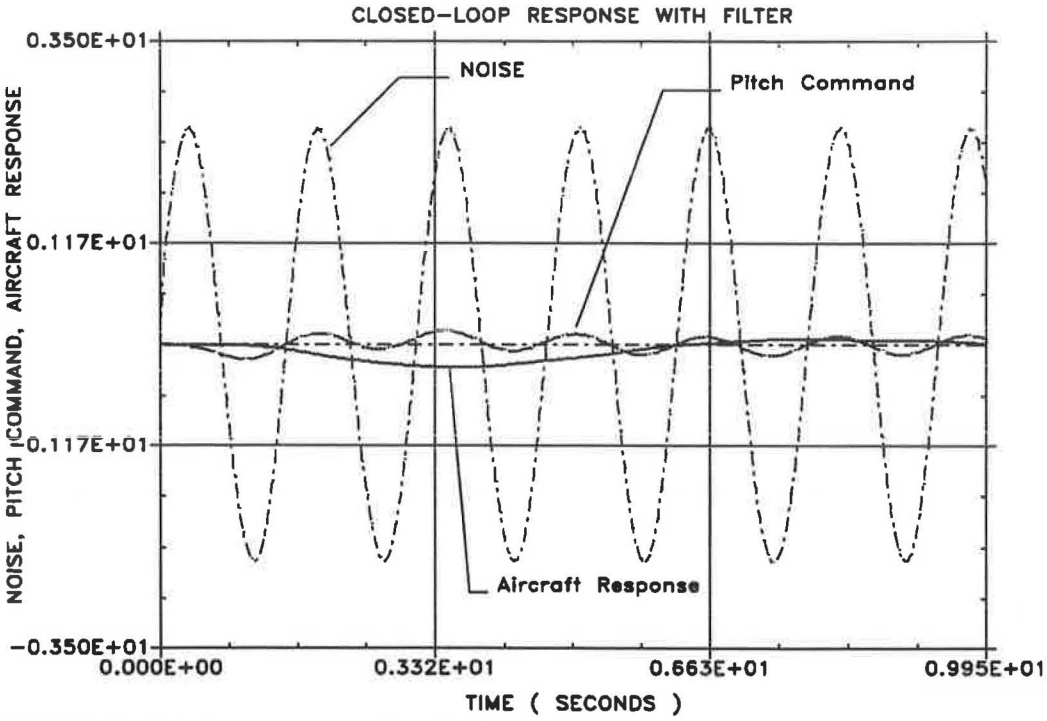

FIGURE 10 Disturbance response with noise filter.

TABLE 1 SUMMARY OF CLOSED-LOOP CHARACTERISTICS OF BODE PLOTS

	Regular Simulation	Noise Filter Simulation
Gain Margin	4.2 dB	4.3 dB
Phase Margin	40 degrees	45 degrees
Bandwidth	1.1 rad/sec	1.2 rad/sec
Maximum Gain	2.5 dB	3.0 dB

TABLE 2 TIME DOMAIN STEP RESPONSE PROPERTIES

	Regular Simulation	Noise Filter Simulation
Overshoot	5.0	8.0
Rise Time	5.0 sec	5.0 sec
Settling Time	20.0 sec	25.0 sec

sible solution, discussed in detail in the following section, is to alter the control loop gains of the PIDDD controller to produce a reduced turbulence response. The gains in the α-β-γ filter can also be changed to provoke similar results. However, one must be careful when altering gains to ensure stable closed-loop behavior.

CONTROL VARIABLE OPTIMIZATION

A proposed technique that allows for the use of the noise rejection filter by reducing the system's turbulence response is an optimization technique that treats the turbulence response of the aircraft as a cost function (performance index) and the controller gains as the variables to be optimized. A gradient direction extremization algorithm is used to formulate the optimization program that calculates the optimal control gains for the landing system. Also, a variety of three-dimensional optimization surfaces that correspond with the cost functions and two independent control variables are constructed to ensure proper operation of the optimization programs. As a result, the turbulence response of the aircraft is examined (employing the optimized control variables) to reveal the improved results when the noise rejection filter is used.

Optimization of Turbulence Response

One of the most straightforward numerical techniques used for optimization with respect to a given cost function is the

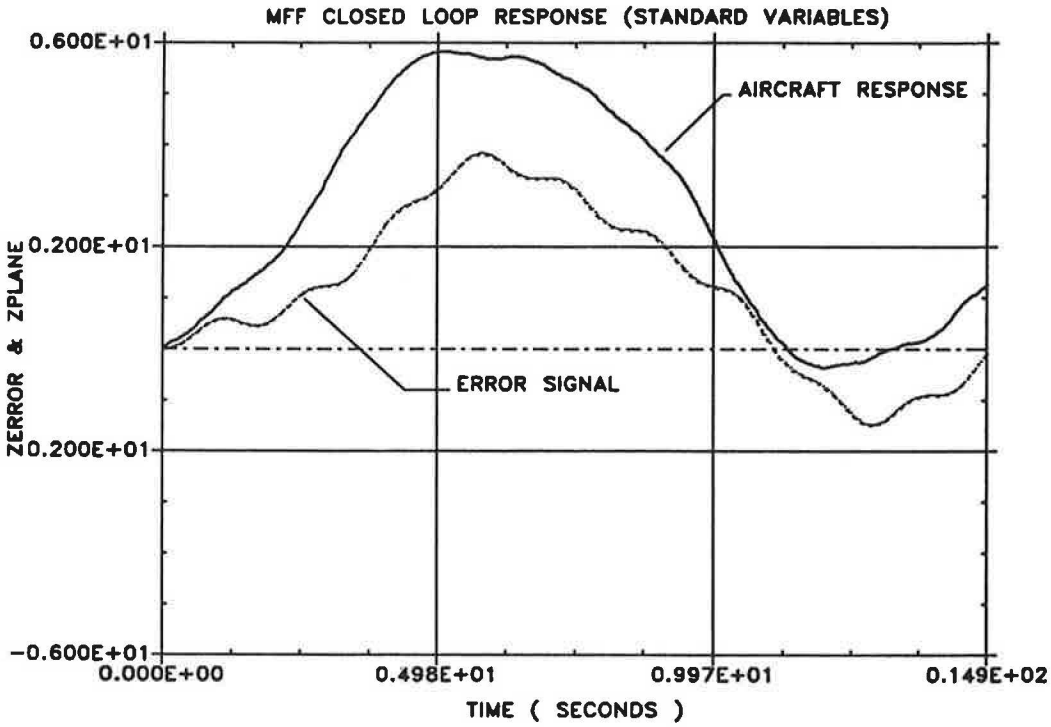

FIGURE 11 Turbulence response with noise filter.

gradient method or method of steepest descent (ascent) (*4*). This method of parameter optimization consists of several consecutive one-dimensional searches of an extremum of a function with respect to a specific cost function. More specifically, the numerical technique moves iteratively in the direction of the gradient, which points locally to the direction of steepest decline (incline) of the respective cost function. A detailed description of the optimization procedure as well as an optimal control representation are given by Bhagavan and Polge (*5*).

The direct application of the gradient direction algorithms for functional extremization varies extensively from problem to problem. For example, the minimization of the turbulence response of an aircraft with respect to its control variables is very unstable in many circumstances. Some of these circumstances include the choice of step size, the time interval used when determining the numerical gradient, and the initial starting guess of the control gains. However, after proper determination of the correct combination of these parameters, the optimization methods converge rather nicely on a minimum.

The cost function is calculated at every iteration to ensure that it is being minimized. The cost function used to describe the turbulence response is illustrated in the following equation. The quadratic form is used to ensure a "well-defined" minimum and also to offset the positive and negative portions of the response.

$$\Phi(\mathrm{x}, t) = \int_{t_0}^{t_f} \mathrm{x}(t)^T \mathrm{x}(t) dt \tag{12}$$

where $\mathrm{x}(t)$ is the position of the aircraft.

This type of cost function, as related to the simulation program, provides for a good convergence rate in the control gains. Other, more complicated cost functions did not produce such stable results.

After implementation of the gradient method optimization program, the results can be summarized in the following manner. First, the optimization program was employed in the ALS computer simulation without the noise filter. Specifically, the two cases considered were (a) minimization of Φ with respect to the derivative and integral gains, and (b) minimization of Φ with respect to the filter gains α, β. Next, the optimization program was used in the ALS computer simulation with the noise rejection filter. The same two cases were considered as in the case without the filter. Illustrations of the optimization surfaces associated with the noise filter closed-loop simulation are given in Figures 12 and 13. The height of the three-dimensional optimization surfaces represents the value of the cost function for the pair of particular independent variables chosen. The two pairs investigated in this paper are integral and derivative controller gains and α and β filter gains.

These particular gains were chosen as optimization variables because the given cost function exhibited high sensitivity to them. For example, varying the double-derivative gain did not affect the magnitude of the cost function to any significant degree. However, the integral and derivative gains affected the cost function very much. For the case including the noise rejection filter, the value of the cost functional for the original gains was 401.4, whereas the optimal gains produced a cost function of 210.7. Therefore, the optimal gains reduced the cost function by approximately 50 percent.

When the α and β filter gains were optimized, the control gains were set to the values optimized. Note that after initial improvements caused by the control gains, additional improvements caused by α and β are minimal.

The minimized turbulence response of the aircraft due to the use of the optimized control and filter gains is now exam-

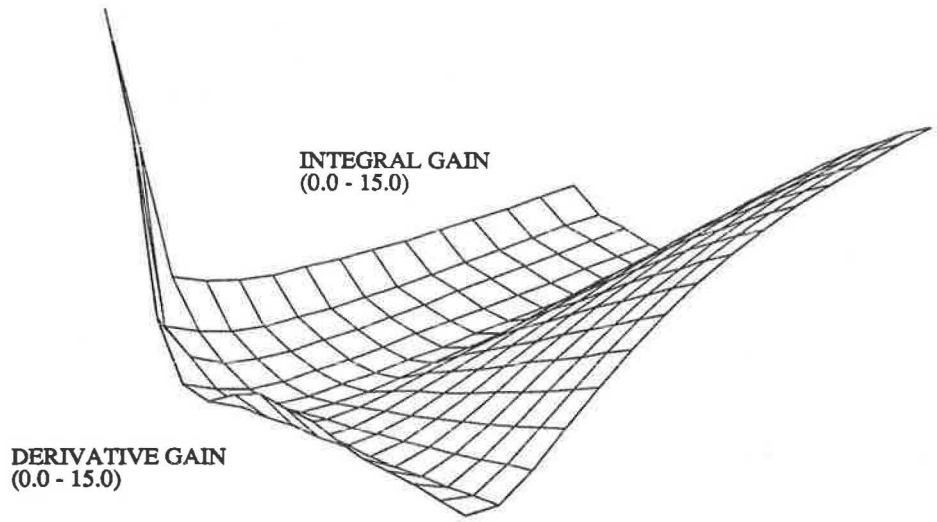

FIGURE 12 Optimization surface for K_I and K_D.

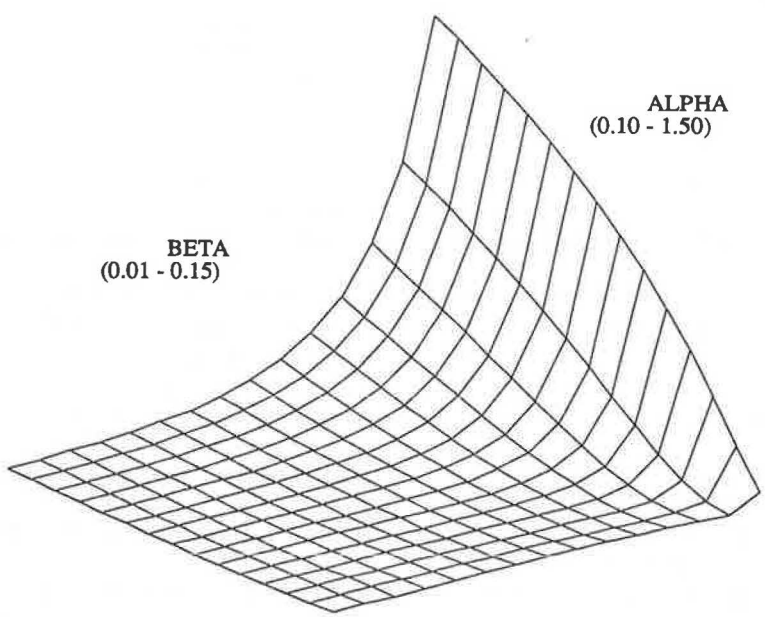

FIGURE 13 Optimization surface for α and β.

ined (Figure 14). In particular, does the implementation of the optimized control and filter gains succeed in improving the turbulence response of the aircraft while continuing to reject noise? The answer to this question is yes. The degree to which the turbulence response is minimized is best described by the figures of the turbulence response of the noise filter system utilizing the original and optimal gains. Note the reduction in both the noise contained in the error signal as compared with the case without the noise filter and also the basic aircraft response.

These results are fine if only the turbulence response is considered. However, this particular change in control/filter gains produces a more oscillatory response for the case of no turbulence. The next section addresses the problem of increased oscillations by optimizing the step response.

Optimization of Step Response

In the previous section, the optimization procedure consisted of minimizing a cost function related to the aircraft's turbulence response with respect to some control variables. However, by simply minimizing a cost function representative of only the turbulence response, the closed-loop characteristics of the ALS can easily be degraded. Therefore, attention is focused on obtaining an optimal step response so that these

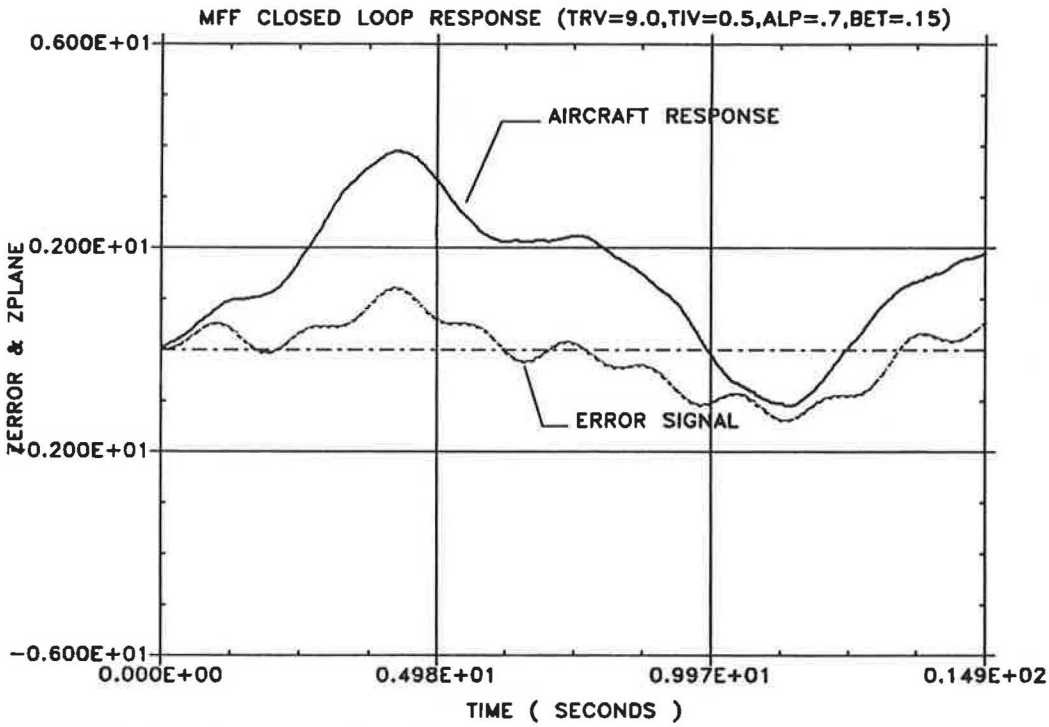

FIGURE 14 Turbulence response for optimal control gains.

TABLE 3 DERIVATIVE AND INTEGRAL GAINS OF OPTIMAL STEP RESPONSE

	Regular Simulation	Noise Filter Simulation
Derivative Gain	1.45	1.32
Integral Gain	16.75	29.52

closed-loop properties are conserved. To obtain an optimal step response, one must produce a fast response time, a low overshoot, and a reasonable settling time. A cost function that takes into account all of the stated requirements for an optimal step response is illustrated below:

$$\Phi(x,t) = \int_{t_0}^{t_f} [1.0 - x(t)]^T [1.0 - x(t)] dt \tag{13}$$

Implementing this cost function in place of the minimal turbulence response cost function will yield the proper control variables for an optimal step response. For the ALS simulations with and without the noise filter the derivative and integral gains of the optimal step response are given in Table 3. The step response with the noise filter is plotted for the original and optimal gains (Figure 15) to illustrate the significant improvements.

Combined Cost Function

Optimizing a cost function that is solely representitive of one particular response often degrades other critical characteristics related to the performance of the ALS. Therefore, the obvious solution is to develop a more encompassing cost function that considers both the turbulence response and the closed-loop characteristics. Because of the two separate parts that would make up such a cost function, each part must be properly weighted to obtain a desired optimal response. The choice of this weighting is left to the discretion of the user. Some examples are given that express the basic ideas of a combined cost function. The first cost function represents the minimization of the turbulence response, and the second represents the best possible step response. To aid in explaining the results more clearly, two tables are formulated. The first table, Table 4, gives the basic results of the uncombined cost functions. Each set of gains from the individual cost functions is then evaluated for the turbulence response and step response. Table 5 combines the preferable qualities from both cost functions and then examines their respective turbulence and step responses. The two gains examined for all cases are derivative and integral control gains. On close examination of the various plots, it can be seen that cases 4 and 7 have good results for both sets of criteria.

CONCLUSIONS

Projected advances in computer technologies coupled with control, filtering, and optimization techniques similar to those

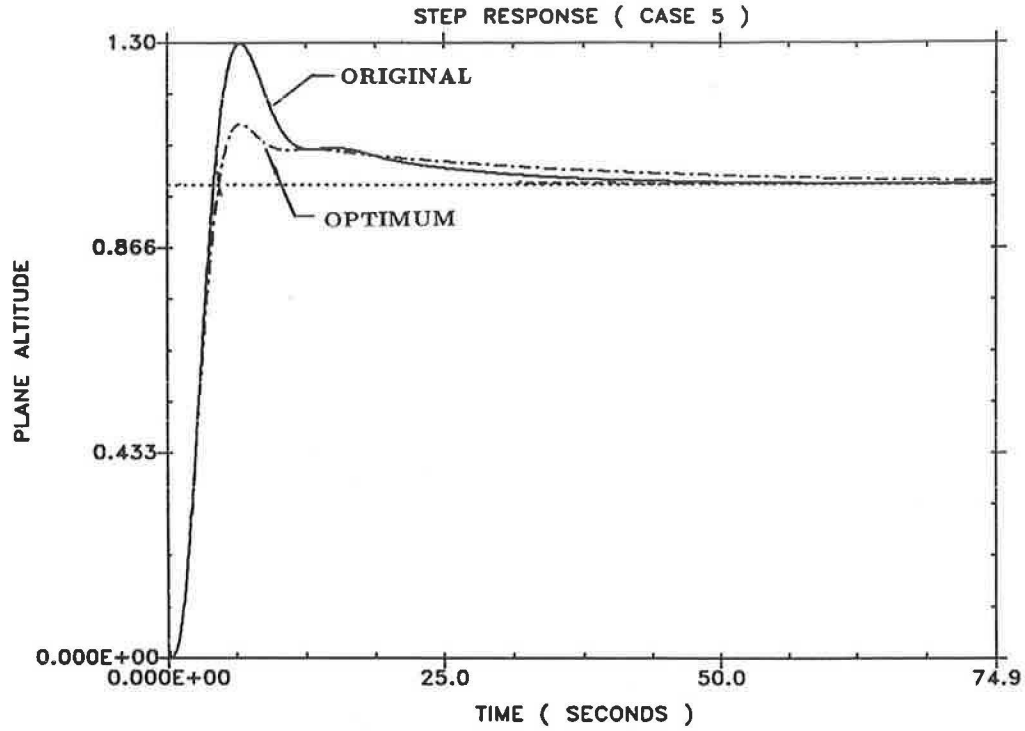

FIGURE 15 Step response comparison for original and optimal gains.

TABLE 4 RESULTS OF UNCOMBINED COST FUNCTIONS

	Gain Type	Gain Values	Turbulence Response	Step Response
Case 1	original gains	derivative = 1.0, integral = 15.0	very poor	good
Case 2	minimum turbulence response gains	derivative = 9.24, integral = 0.91	very good	very poor
Case 3	minimum step response gains	derivative = 1.32, integral = 29.52	very poor	very good

TABLE 5 RESULTS OF COMBINED COST FUNCTIONS

	Gain Values	Turbulence Response	Step Response
Case 4	derivative = 4.0, integral = 21.0	good	good
Case 5	derivative = 2.0, integral = 5.0	poor	very poor
Case 6	derivative = 8.0, integral = 25.0	good	poor
Case 7	derivative = 3.0, integral = 10.0	good	good
Case 8	derivative = 7.0, integral = 10.0	good	poor

presented here will become significant in the design of future ALSs for commercial aircraft. An ALS was simulated and analyzed so that improved performance with respect to radar tracking and control could be evaluated. Using a simplified model with robust tracking and control strategies, the noise sensitivity of the closed-loop simulation was examined. A noise rejection filter was introduced that produced excellent noise rejection abilities, but at the cost of an increased turbulence response of the aircraft. To address this dilemma, an optimization program was developed that minimized the turbulence response of the aircraft with repsect to some of the control and filter variables of the ALS. This optimization produced the optimal control and filter gains of the ALS with respect to a cost function related to the turbulence and step responses. Employing these optimal gains in the ALS control and filter algorithms produced improved results for the goal of rejecting radar noise while preserving a normal turbulence response.

ACKNOWLEDGMENTS

This paper was written for the Graduate Research Award Program on Public-Sector Aviation Issues sponsored by FAA and administered by TRB.

The author would like to thank D. Joseph Mook, assistant professor of mechanical engineering, State University of New York at Buffalo; E. Thomas Burnard and Larry Jenney of TRB; Greig W. Harvey, assistant professor of civil engineering, Stanford University; and Agam N. Sinha, head, transportation and data systems, MITRE Corporation, for their support, help, and encouragement throughout this project.

REFERENCES

1. A. N. Sinha. The Realization of Microwave Landing System Benefits. Presented at the PLANS 1988 Conference, Orlando, Fla, 1988.
2. J. N. Barrer and A. N. Sinha. An Operational Perspective of Potential Benefits of Microwave Landing Systems. *Proc. 31st Annual Meeting of the Air Traffic Control Association*, Arlington, Va., 1986.
3. M. J. Roemer. An Automatic Carrier Landing System Simulation/Realization with Control Variable Optimization. Master's thesis. University of Buffalo, N.Y. Feb. 1989.
4. D. Andrisani, F. P. Kuhl, and D. Gleason. A Nonlinear Tracker Using Attitude Measurements. *IEEE Transactions on Aerospace and Electronic Systems*, Vol. AES-22, No. 5, Sept. 1986, pp. 574–580.
5. B. K. Bhagavan and R. J. Polge. Performance of the g-h Filter for Tracking Maneuvering Targets. *IEEE Transactions on Aerospace and Electronic Systems*, Vol. AES-10, No. 6, Nov. 1974, pp. 721–727.
6. R. J. Fitzgerald. Simple Tracking Filters: Steady State Filtering and Smoothing Performance. *IEEE Transactions on Aerospace and Electronic Systems*, Vol. AES-16, No. 3, Nov. 1980, pp. 860–864.
7. A. Gelb, ed. *Applied Optimal Estimation*. MIT Press, Cambridge, Mass., 1984.
8. F. L. Lewis. *Optimal Estimation*. Wiley-Interscience, New York, 1986.
9. J. B. Pearson. Kalman Filter Applications In Airborne Radar Tracking. *IEEE Transactions on Aerospace and Electronic Systems*, Vol. AES-10, No. 3, May 1974, pp. 685–691.
10. R. J. Fitzgerald. Simple Tracking Filters: Closed Form Solutions. *IEEE Transactions on Aerospace and Electronic Systems*, Vol. AES-17, No. 6, Nov. 1981, pp. 781–785.
11. A. P. Sage and C. C. White. *Optimum Systems Control*, Prentice Hall, Inc., Englewood Cliffs, N.J., 1977.
12. J. P. Schwieterman. Airline Routes and Metropolitan Areas: Changing Access to Non-stop Service Under Deregulation. In *Transportation Research Record 1161*, TRB, National Research Council, Washington, D.C., 1988, pp. 1–13.
13. I. H. Shyu. Performance Analysis of Several Aircraft Tracking Filters. Master's thesis. University of Buffalo, N.Y. Aug. 1988.
14. R. A. Singer. Estimating Optimal Tracking Filter Performance for Maneuvering Targets. *IEEE Transactions on Aerospace and Electronic Systems*, Vol. AES-6, No. 4, July 1970, pp. 432–439.
15. C. T. Villarreal. Uses and Misuses of Risk Metrics in Air Transportation. In *Transportation Research Record 1161*, TRB, National Research Council, Washington, D.C., 1988, pp. 31–42.